SISAL FIBER-REINFORCED GEOPOLYMER COMPOSITES: TAILORING DURABILITY VIA MATRIX COMPOSITION

HENRIQUE ALMEIDA SANTANA, CLEBER MARCOS RIBEIRO DIAS

Federal University of Bahia – Rua Aristides Novis 02, Federação. 40210-630, Salvador/BA, Brazil.

ABSTRACT

This study explores the impact of different alkaline activators and matrix dosages (low vs. high free ion concentration) on the durability of sisal fiber-reinforced alkali-activated composites. Samples from various composite groups were exposed to outdoor weathering for six months, while control specimens were maintained under laboratory conditions. Durability was assessed using three-point bending tests to measure specific energy as an indicator of degradation. Additionally, scanning electron microscopy (SEM) was employed to examine the fractured surfaces. The mechanical tests revealed a substantial reduction in specific energy—up to 55.82%—in composites with high free ion concentration that were exposed to outdoor conditions for six months. SEM analysis further identified voids at the fiber-matrix interface in composites with high free ion content. These findings indicate that, when improperly dosed, geopolymer matrices can degrade vegetable fibers regardless of environmental exposure or the type of alkali activator used. Optimizing the free ion content during matrix formulation can mitigate or even prevent this degradation.

KEYWORDS:

Durability; cellulose; alkaline hydrolysis; sisal fiber.

1. INTRODUCTION

Geopolymers can exhibit physical and mechanical properties comparable to Portland cement while generating lower carbon dioxide (CO_2) emissions throughout their production cycle (Provis et al., 2014). However, geopolymers are prone to brittle fractures (Yan et al., 2016), characterized by low energy absorption typical of ceramic materials, which necessitates reinforcement to overcome this limitation. Vegetable fibers have generated significant interest as potential reinforcements in geopolymer matrices. The advantages of vegetable fibers include their lower density compared to steel and glass fibers, renewable resources, availability in developing countries at a relatively low cost, and their diverse morphological and dimensional variety (Ferreira et al., 2015). Nonetheless, a recent literature review by Santana et al. (2021) emphasized that the durability of vegetable fibers has yet to be thoroughly investigated, a critical concern given the fragile physical and chemical stability of these fibers in an alkaline environment.

It is well established that Portland cement-based matrices can degrade vegetable fibers over time through two primary mechanisms that compromise fiber durability: alkaline hydrolysis and mineralization, both of which are associated with the by-products of Portland cement hydration (Wei and Meyer, 2015). Notably, hydrated calcium silicate (C-S-H) and portlandite (CH) are the primary products formed during Portland cement hydration (Gallucci and Scrivener, 2007). In contrast, geopolymers, which are binders based on aluminosilicate precursors, involve different chemical reactions (Provis and Bernal, 2014). During geopolymerization, the presence of a specific oxide "M" (such as Na_2O or K_2O) leads to the formation of M-A-S-H (M-aluminosilicate hydrate). In systems with calcium-rich precursors, calcium oxide (CaO) can result in the formation of C-A-S-H gel (calcium aluminosilicate hydrate). Consequently, mechanisms developed to mitigate the degradation of vegetable fibers

in Portland cement matrices are unlikely to be effective for geopolymers, since the phases formed in these matrices are not the same.

The production of composites based on vegetable fibers and geopolymer matrices is constrained by the durability of this material. Understanding the behavior of fibers within geopolymer matrices is essential, particularly in light of climatic influences for assessment that can predict long-term performance. To address this, the interaction between vegetable fibers and geopolymer binders was thoroughly studied by evaluating composites produced with different alkaline activators after exposure in a natural laboratory environment and in a natural, outdoor environment.

2. METHODOLOGY

2.1 Fiber characterization

The sisal vegetable fibers were previously washed in distilled water at 50°C and dried in an oven at 80°C for 48 hours to remove superficially impregnated impurities (sugar, starch, proteins, oil and wax), which helps preserv fiber-matrix adhesion. The fibers have a skeletal density of 1.59 ± 0.04 g/cm², as determined by a helium gas pycnometer (AccuPyc II 1340 Micromeritics); a crystallinity degree of 70%, determined by X-ray diffraction, with diffraction spectra obtained over a scanning range (2θ) from 5° to 50°. The tensile strength of the fibers is 466.86 ± 95.66 MPa, determined from stress-strain curves in accordance with ASTM C1557 (2008) method. It is important to note that, as a natural material, sisal fibers present dimensional variability and defects, which explains the variation observed in tensile strength.

2.2 Dosage and characterization of the matrix

To evaluate the impact of dosage efficiency in alkali-activated matrices on fiber durability, predictive models for properties were utilized, as outlined in a previous study (Santana et al., 2023). These models were developed using i-Optimal statistical mixture design. Consequently, four formulations of geopolymeric matrix were established based on boundary conditions:

i) Na_{min} –activated with sodium silicate solution, optimized to minimize the concentration of free alkali ions in the pore solution;
ii) Na_{max} –activated with sodium silicate solution, optimized to maximize the concentration of free alkali ions in the pore solution;
iii) K_{min} –activated with potassium silicate solution, optimized to minimize the concentration of free alkali ions in the pore solution;
iv) K_{max} –activated with potassium silicate solution, optimized to maximize the concentration of free alkali ions in the pore solution.

Metacaulim HP Ultra (MK) from *Metacaulim do Brasil,* and thermally treated asbestos-cement waste (ACW_T) were used as precursors. The ACW_T was meticulously treated according to the methodology described by Carneiro et al. (2021). The activating solutions were prepared with densified silica fume provided by *Companhia de Ferro Ligas da Bahia*, along with sodium hydroxide (NaOH), and potassium hydroxide (KOH), both with 98% purity. Table 1 presents the skeletal densityof metakaolin, silica fume, and ACW_T, determined using a helium gas pycnometer (AccuPyc II 1340 Micromeritics), along with their specific surface area measured by the BET method on a Gemini VII Micromeritics Pycnometer, and chemical composition, obtained through X-ray fluorescence using a Bruker S2 Ranger spectrometer. The median of particle equivalent diameter (D_{50}) of the precursor materials was determined by dry laser diffraction using a particle size analizer S3500 Microtrac.

Metakaolin is primarily composed of alumina and silica, which are essential for the formation of M-A-S-H. In contrast, ACW_T is rich in calcium, which can promote the formation of C-A-S-H, C-S-H, and portlandite. The selection of these two precursors with distinct chemical compositions was driven by the need to evaluate the durability of vegetable fibers in the presence of various compounds.

Sodium and potassium silicate solutions were prepared in the laboratory to assess the influence of alkaline bases (NaOH or KOH) on the durability of vegetable fibers. Liquid sodium silicate (LSS) was synthesized using 52%

deionized water, 27% silica fume (SF), and 21% sodium hydroxide (NaOH) by mass, resulting in a molar ratio SiO_2/Na_2O of 1.33. Liquid potassium silicate (LKS) was produced with 49% deionized water, 27% SF, and 24% potassium hydroxide (KOH) by mass, yielding a molar ratio SiO_2/K_2O of 1.16. These silicate solutions were prepared with different compositions because NaOH showed greater efficiency in precursor material decomposition reactions in preliminary laboratory tests. The activating solution materials were manually mixed, sealed with plastic film, and allowed to cool to room temperature before use.

Table 1 - Chemical composition and physical properties of materials.

Materials	Metakaolin	ACW_T	Silica fume
Physical properties			
Skeletal density (g/cm^3)	2.80	2.95	2.32
BET specific surface area (m^2/g)	30.52	6.68	15.15
D_{50}	20.29	18.80	-
Chemical composition (%)			
SiO_2	44.88	18.20	81.75
Al_2O_3	42.86	4.06	1.41
Fe_2O_3	4.82	2.35	4.90
MgO	0.67	7.27	1.34
CaO	-	48.69	0.29
Others	2.54	3.13	5.91
Loss on ignition (1000 °C)	4.23	16.30	4.40

The compressive strength (C_S) of the pastes was determined on three cubic specimens with 40 mm of edge, per formulation, after 28 days of curing in an environment with a temperature of (25 ± 2) °C and relative humidity of (65 ± 5) %. Testing was conducted using a servo-hydraulic press with a capacity of 1200 kN at a loading rate of 500 N/s. Paste density (ρ) was measured using a helium gas pycnometer (AccuPyc II 1340 Micromeritics). Control of free alkali ions in the pore solution of the matrix was indirectly achieved by measuring the electrical conductivity (σ) of the residual solution obtained after immersing samples in distilled and deionized water (see details at Santana et al., 2023). The mass fractions and characteristics of the formulations are presented in Table 2.

Table 2 - Formulations of alkali-activated matrices used in the exposure test.

Formulation	Weight fraction			Properties		
	MK	ACW_T	Activator	C_S (MPa)	ρ (g/cm^2)	σ (mS/cm)
Na_{min}	0.474	0.013	0.513	60.35 ± 1.81	2.35 ± 0.006	7.88
Na_{max}	0.286	0.127	0.586	40.42 ± 0.55	2.14 ± 0.003	28.60
K_{min}	0.490	0.000	0.510	57.36 ± 2.89	2.44 ± 0.017	7.58
K_{max}	0.252	0.148	0.600	33.55 ± 0.03	2.25 ± 0.017	28.50

2.3 Production and aging of the composites

For the production of the composites, fibers were cut to a length of 25 mm, the critical length determined in preliminary laboratory tests. A fiber content of 2.5% by mass of the precursor was used, determined as the maximum proportion that did not compromise the workability of the mixture. The four pre-dosed pastes were prepared in a 5 L planetary mixer. Initially, metakaolin and ACW_T were mixed for 30 seconds, followed by the addition of the activating solution, with mixing continued for another 30 seconds. The mixture was then blended for an additional 30 seconds. Next, the mixer was paused for 30 seconds to scrape down the sides of the bowl and the mixer paddle. After this, the mixer was restarted, and sisal fibers were added to the mixture, which was then mixed for another 30 seconds to ensure uniform fiber distribution. The entire process was carried out at a low speed (62.5 ± 5 rpm).

The composites were molded into prismatic forms with internal dimensions of 230 mm x 50 mm x 10 mm, ensuring a homogeneous and well-dispersed fiber distribution. The molds were kept in a laboratory environment at (25±2) °C and (65±5) % relative humidity for 24 hours before being demolded and placed in the exposure environment. Figure 1 presents the outdoor exposure conditions for the three groups of composites under study.

Three composites from each group were evaluated after 120 days of laboratory exposure (120Lab series) and after 120 days of natural exposure aging (120Nat series). All groups were kept in the laboratory for 28 days prior to exposure to ensure the completion of all alkali-activation reactions.

The samples were exposed on the terrace of the School of Engineering at the Federal University of Bahia, Brazil, located at latitude 12° 59 '58.30 " S and longitude 38° 30' 37.07" W, according to the WGS 84 geodetic reference system. Based on the methodologies of Tanaca et al. (2012), and Almeida et al. (2013), the specimens were placed on galvanized steel supports, facing true north, with a 45° inclination relative to the horizontal plane.

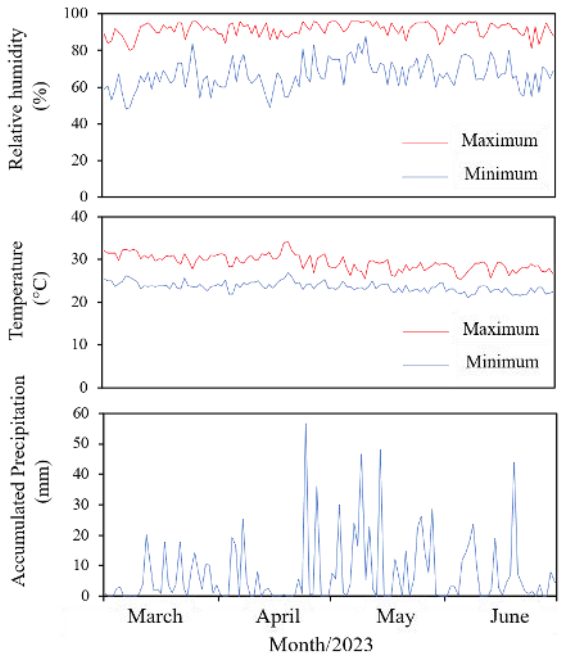

Figure 1 - Exposure conditions for the three groups of composites under study.

2.4 Composites evaluation

To determine the mechanical properties of composites, a three-point bending test was performed with a span of 170 mm, using a displacement rate of 0.5 mm/min. The tests were conducted on an INSTRON universal testing machine, model 23-10, equipped with a 2 kN load cell. The limit of proportionality (LOP) of the composites was determined from the load (N) versus deflection (mm) curve, as calculated using Equation 1.

$$LOP = \frac{F_f L}{wh^2} \qquad \text{(Eq. 1)}$$

Where F_f is the load at the point on the load-deflection curve where behavior becomes nonlinear (N), L is the span (170 mm), w is the width, and h is the height of the cross-sectional area of the sample (mm).

The absorbed energy during the test was determined by integrating the load versus deflection curve. The specific energy (SE) was determined at different deflection levels by the ratio of absorbed energy to the cross-sectional area of the samples:

(i) $SE_{(0\text{-}1)}$ level between 0 and 1 mm of deflection, referring to the region before any cracking occurs, where the transfer of elastic stress is the dominant mechanism and longitudinal displacements of the fiber and matrix at the interface are geometrically compatible;

(ii) $SE_{(1\text{-}9)}$ level between 1 and 9 mm of deflection, referring to the region characterized by the appearance of multiple cracks supported by fiber anchoring. Subsequently, existing cracks begin to open, supported by the fiber length (25 mm). This widening is intensified at the central crack in the direction of the flexural load application;

(iii) $SE_{(10\text{-}20)}$ level between 10 and 20 mm, referring to the region where the bonds between fibers and the matrix are broken, resulting in a decrease in load with an increase in deflection of the composites.

The microstructure of the polished sections obtained from the fractured region of the composites was examined using a Hitachi TM3030 scanning electron microscope, operating at an acceleration voltage of 15 kV. To ensure conductivity for analysis, a thin carbon layer was applied to the samples. Additionally, the polished section were analysed after being embed in a polymer resin, allowing for detailed observation of the interface zone between the matrix and the sisal fibers.

3. RESULTS

3.1 Mechanical tests

Figure 2 shows the load versus deflection curves of the composites after exposure in the laboratory environment for 120 days (120Lab) and after exposure in the natural environment for 120 days (120Nat).

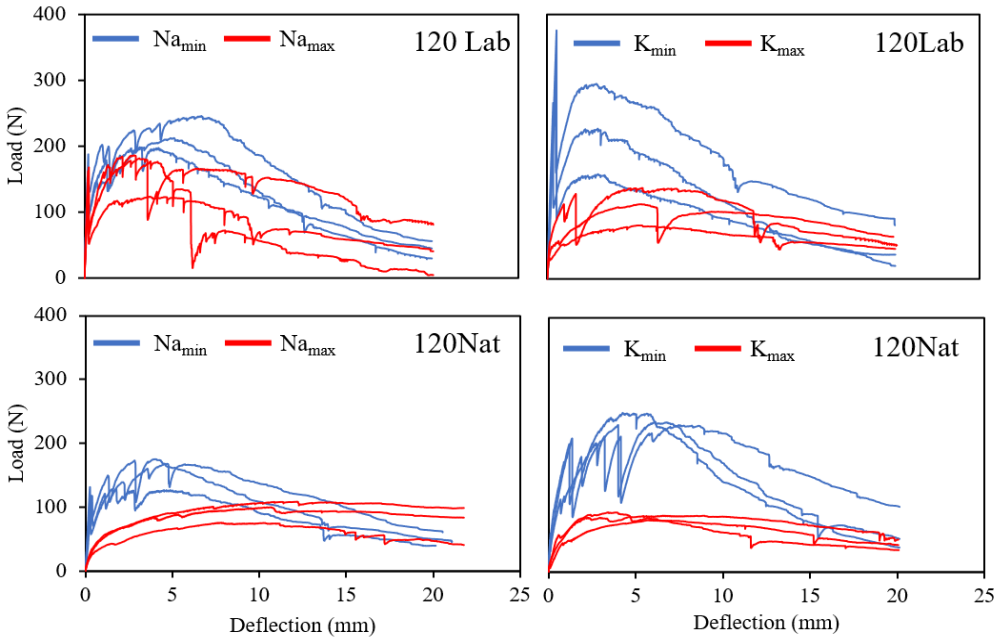

Figure 2 – Load-deflection curves for composite series: laboratory (120Lab) and outdoor exposure (120Nat).

Na_{max} and K_{max} composites exposed to natural weathering did not exhibit well-defined first crack peaks. These composites were subjected to intense daily cycles of wetting and drying due to frequent precipitation during the exposure period (as shown in Fig. 2). Such conditions, as discussed by Juarez et al. (2007), can cause variations in humidity and temperature, leading to cracks and microcracks from dimensional changes in the composite. This suggests that the matrices were already cracked at the beginning of the test, with the fibers temporarily bearing the applied load.

After mixing, vegetable fibers tend to absorb water, which can contribute to matrix shrinkage and weaken the adhesion between the composite phases (Ferreira et al., 2020). This effect is particularly significant for Na_{max} and K_{max} composites, which contain a higher proportion of liquid in their compositions. Additionally, Ballesteros et al. (2019) highlight that vegetable fibers are hydrophilic, leading to incompatibility and reduced adhesion at the fiber-matrix interface, a problem that may be exacerbated by the higher porosity of these composites.

The geopolymeric composites reinforced with vegetable fibers exhibited the characteristic behaviour of a Portland cement-based composite reinforced with vegetable fiber, as presented by Melo Filho et al. (2013). The curves obtained in the three-point bending test allowed for the determination of the limit of proportionality (LOP) and the specific energy (SE) of the samples.

3.1.1 Limit of proportionality (LOP)

Figure 3 presents the LOP values obtained from the load versus deflection curves of the composites, highlighting the influence of both the exposure environment and the matrices on the observed values.

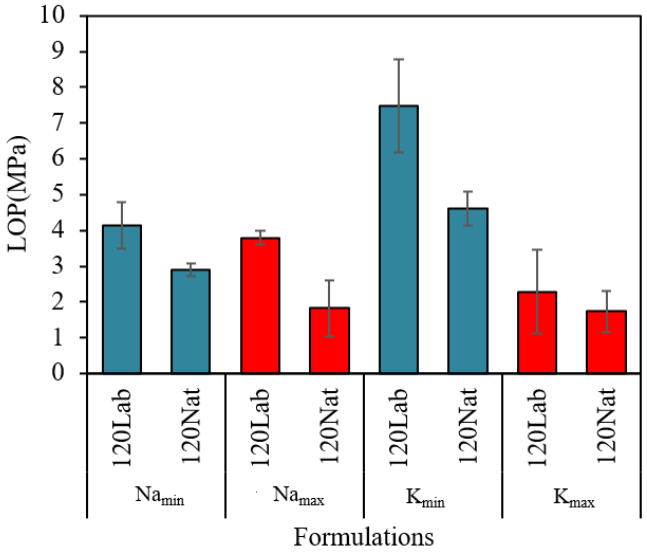

Figure 3 – Limit of proportionality of the composite series.

For composites produced with sodium-based matrices, LOP was higher for composites maintained in a laboratory in comparison to that exposed to the weathering, being 8.5% higher for Na_{min} and 36.9% higher for Na_{max}. This behavior can also be explained by the weakening of the matrix caused by drying shrinkage over time, described in the literature as a common problem in geopolymer matrices (Amorim Junior et al., 2021; Zhang et al., 2022) or by matrix leaching, caused by climate variations. Additionally, the vegetable fiber may weaken due to alkaline hydrolysis (Wei and Meyer, 2015), a process intensified by moisture in the natural environment and dimensional changes in the fibers (Melo Filho et al., 2013). This weakening can lead to internal stresses within the matrix or results in discontinuities following degradation.

Similar behaviour was observed for the potassium-based matrices, with emphasis on the high LOP value determined for 120Lab. This group exhibited well-defined first crack load peaks, characterized by a single crack opening in the center of the composite and a sudden transfer of load from the matrix to the fibers in that region.

Prior to cracking, the bond between the fiber and the matrix was maintained through chemical adhesion and friction, likely contributing to the load peak. The abrupt transfer of high stress from the matrix to the fiber may have exceeded the shear strength between these two materials, causing a sudden reduction in the load. However, the load was subsequently recovered, indicating that the fibers were still capable of bearing loads even after 120 days within the matrix.

3.1.2 specific energy (SE)

Regarding specific energy (Figure 4), the initial deflection level (SE_{0-1}), primarily influenced by the matrix, demonstrates superior values for the Na_{min} and K_{min} composites produced with matrices optimized with higher compressive strength, lower porosity, and minimized free alkali content.

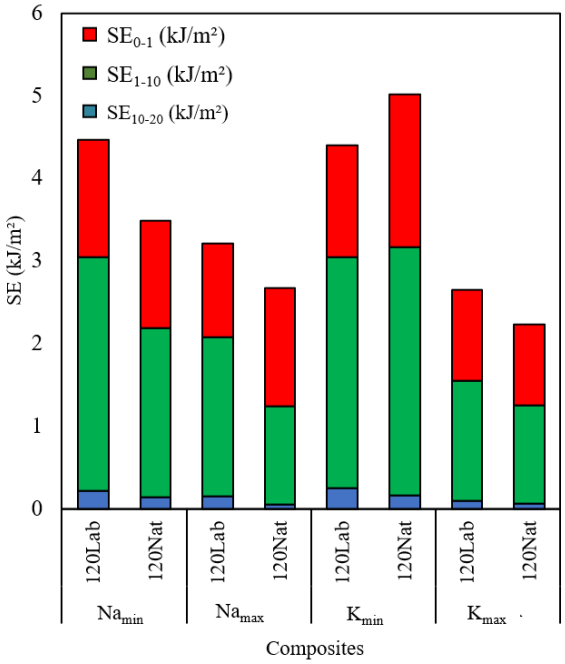

Figure 4 – Specific energy determined for the groups of composites evaluated.

The specific energy of the second level (SE_{1-10}) reflects the fiber's capacity to absorb energy post-matrix rupture. It indicates fiber-matrix bond strength and fiber degradation due to free alkali exposure. As expected, the SE_{1-10} values were also higher for the Na_{min} and K_{min} composites. Notably, the SE_{1-10} value for K_{min} at 120Nat (2.99 kJ/m²) was 31.7% higher than the value obtained for the Na_{min} composite under the same conditions, highlighting K_{min} superior performance even under severe environmental condition (120Nat). Even after 120 days of outdoor exposure, the K_{min} exhibited only 3 or 5 matrix cracks marked by the abrupt load reduction in the three-point bending test). Following the crack formation, the composite regained load-bearing capacity, surpassing initial levels.

Another crucial factor influencing composite specific energy is the fiber critical length. As Bentur and Mindess (2006) noted, fibers shorter than the critical length cannot generate sufficient stress to reach their tensile strength, limiting their effectiveness. Conversely, fibers exceeding the critical length can develop full tensile stress, maximizing their potential.

According to the load versus deflection curves of the evaluated composites, the critical length can vary depending on the properties of the matrix and the exposure environment. In a preliminary study, the critical length was determined for the Na_{min} matrix through pull-out tests and adopted for the other composites. The behaviour of the composite produced with the same Na_{min} matrix after 120Nat suggest that a longer fiber length might be necessary to offset the loss of specific energy due to reduced interfacial adhesion.

.

Finally, it is noteworthy that for the Na_{max} and K_{max} composites, after 120 days in the natural environment, the specific energy values for the last deflection level (SE_{10-20}) are close to SE_{1-10}. In fact, the stress-strain curve for these composites shows a constant behaviour without significant variations in the supported load, indicating that the fibers are easily pulled out from the matrix and the bond strength is ineffective. Adhesive strength is compromised when fibers are gradually degraded, affecting the bond with the matrix and forming voids at the interface zone.

3.2 Microstructural analysis by SEM

Figure 5 and Figure 6 present micrography of polished sections of the composites after aging in the laboratory and outdoor exposure, respectively.

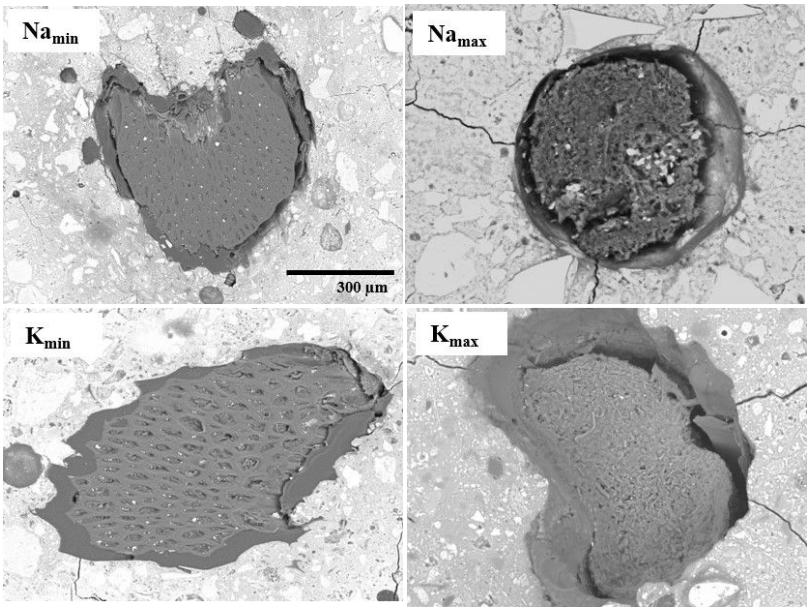

Figure 5 – Microstructural analysis of polished sections in fractured regions of composites exposed to 120Lab.

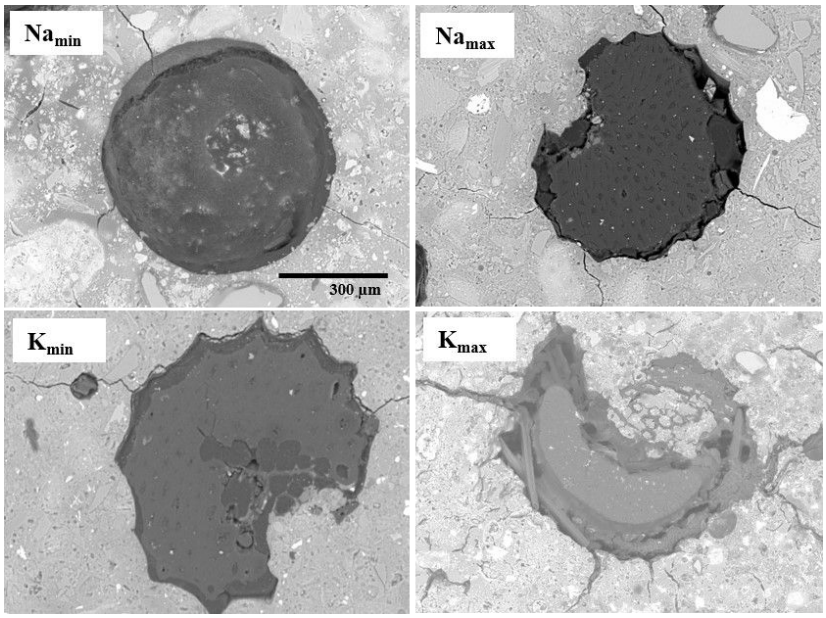

Figure 6 – Microstructural analysis of polished sections in fractured regions of composites exposed to 120Nat.

Notably, all composites exhibit voids in the matrix-fiber interface zone, likely caused by the bending test, where fibers were partially pulled out after the applied stress on the composite exceeded the fiber-matrix adhesion strength.

The dimensions of the voids can be considered indicative of the intensity of degradation in the interface region between the fiber and the matrix. It is observed that the decomposition affects the outermost layers, primarily composed of amorphous and alkaline-sensitive components such as lignin and hemicellulose. Wei and Meyer (2015) observed analogous behavior in analyses of fractured sections of Portland cement-based composites reinforced with vegetable fibers.

For both environments evaluated, it is noted that in composites produced with optimized matrices with maximized free alkali ions (Na_{max} and K_{max}), the space between the matrix and the fiber is larger, probably due to the greater availability of free alkalis in this region, promoting physical and chemical reactions between the composite components. Additionally, the results align with a three-point bending test conducted on the composite, where matrices dosed with minimized free alkaline ions (Na_{min} and K_{min}) did not exhibit significant toughness losses after composite aging.

It is also noteworthy that the fibers appear more intact for composites exposed to the natural environment and produced with N_{amin} and K_{min} matrices compared to composites exposed in the laboratory environment. While weathering in the natural environment can have adverse effects, causing dimensional variations in fibers and potentially enhancing void formation at the interface zone, it can also have positive effects by leaching free alkalis or promoting unintentional fiber hornification through observed wetting and drying cycles, as shown in **Figure 1**.

4. CONCLUSIONS

To assess the durability of vegetable fibers in geopolymer matrices, composites were produced using matrices with various alkaline bases and exposed to both natural and laboratory environments. Analysis revealed the following:

Vegetable fibers impart ductile behaviour to geopolymer binders, absorbing energy post-crack. This behaviour is influenced by matrix alkalinity and exposure environment. Composites with optimized matrices, characterized by minimal free ions and laboratory exposure, exhibited superior performance.

K_{min} matrix composites demonstrated notable recovery and increased load-bearing capacity following the first crack, suggesting that fiber degradation did not compromise their anchoring function within the matrix, regardless of environment or exposure duration.

Mechanical results aligned with microstructural observations, revealing voids in the interface zone, particularly pronounced in Na_{max} and K_{max} outdoor exposed composites. These voids indicate degradation of the outer fiber layers, such as amorphous components susceptible to alkaline hydrolysis, including hemicellulose and lignin.

Combined analysis suggests that controlling matrix aggressiveness is a promising strategy for effective fiber integration.

ACKNOWLEDGEMENTS

The authors would like to acknowledge the financial support of CNPq (Process n° 309270/2022-7), FAPESB (Process n° 0486/2020) and CAPES (Process n° 88887.838290/2023-00). The authors also acknowledge the *Laboratório de Ensaios em Durabilidade dos Materiais* (LEDMa) of the *Universidade Federal da Bahia*, where the material characterization tests were carried out.

REFERENCES

Almeida, A. E. F. D. S.; Tonoli, G. H. D.; Santos, S. F. D.; Savastano Jr, H. Improved durability of vegetable fiber reinforced cement composite subject to accelerated carbonation at early age. **Cement and Concrete Composites**, v. 42, p. 49-58, 2013.

ASTM C1557, Standard Test Method for Tensile Strength and Young's Modulus of Fibers. West Conshohocken, PA, USA: American Society for Testing and Materials; 2008.

Bentur, A.; Mindess, S. Fibre reinforced cementitious composites. Crc Press, 2006.

Carneiro, G. O.; Santos, T. A.; Simonelli, G.; Ribeiro, D. V.; Cilla, M. S.; Dias, C. M. Thermal treatment optimization of asbestos cement waste (ACW) potentializing its use as alternative binder. **Journal of Cleaner Production**, v. 320, p. 128801, 2021.

Ferreira, S. R.; de Andrade Silva, F.; Lima, P. R. L.; Toledo Filho, R. D. Effect of fiber treatments on the sisal fiber properties and fiber–matrix bond in cement based systems. Construction and Building Materials, v. 101, p. 730-740, 2015.

Gallucci, E.; Scrivener, K. Crystallisation of calcium hydroxide in early age model and ordinary cementitious systems. **Cement and Concrete Research**, v. 37, n. 4, p. 492-501, 2007. https://doi.org/10.1016/j.cemconres.2007.01.001

Melo Filho, J. A.; De Andrade Silva, F.; Toledo Filho, R. D. Degradation kinetics and aging mechanisms on sisal fiber cement composite systems. Cement and Concrete Composites, v. 40, p. 30-39, 2013.

Provis, J. L; Bernal, S.A. Geopolymers and related alkali-activated materials. **Annu. Rev. Mater. Res.**, v. 44, p. 299-327, 2014. https://doi.org/10.1146/annurev-matsci-070813-113515

Santana, H. A.; Júnior, N. S. A.; Ribeiro, D. V.; Cilla, M. S.; Dias, C. M. Vegetable fibers behavior in geopolymers and alkali-activated cement based matrices: A review. **Journal of Building Engineering**, v. 44, p. 103291, 2021.

TANACA, H. K.; DIAS, C. M. R.; GAYLARDE, C. C.; JOHN, V. M.; SHIRAKAWA, M. A. Discoloration and fungal growth on three fiber cement formulations exposed in urban, rural and coastal zones. **Building and Environment**, v. 46, n. 2, p. 324-330, 2011.

Wei, J.; Meyer, C. Degradation mechanisms of natural fiber in the matrix of cement composites. **Cement and concrete Research**, v. 73, p. 1-16, 2015.

Yan, L.; Kasal B.; Huang, L. A review of recent research on the use of cellulosic fibres, their fibre fabric reinforced cementitious, geo-polymer and polymer composites in civil engineering. **Composites Part B: Engineering**, v. 92, p. 94-132, 2016. https://doi.org/10.1016/j.compositesb.2016.02.002